Hypothesis

A structural and dynamic molecular model for the sodium channel of *Electrophorus electricus*

Edward M. Kosower

Department of Chemistry, Sackler Faculty of Exact Sciences, Tel-Aviv University, Ramat-Aviv, 69978 Tel-Aviv, Israel and *Department of Chemistry, State University of New York, Stony Brook, NY 11794, USA*

Received 10 January 1985

Chemical logic and single group rotation (SGR) theory are applied to the primary structure determined by Noda et al. [(1984) Nature 312, 121–127] to construct a molecular model of the sodium channel of *Electrophorus electricus*. Both structural and dynamic aspects of the channel are accounted for, including gating current, sensitivity to changes in membrane potential, channel opening, a binding site for sodium, selectivity for sodium over potassium, capacity for rapid sodium flow, sensitivity to batrachotoxin (or other toxins) and inactivation.

1. INTRODUCTION

1.1. *Brief background*

In many cases, the sodium channel is the central element in the transfer of integrated information from the dendrites and cell body of neurons through the axon. The transfer signal is an action potential propagated through the axon and arises from the operation of the sodium and potassium channels of the axon. A deep understanding of the functioning of channels or receptors and other biological polymers cannot be achieved without knowledge about the molecular structure [1].

The sodium channel is a glycoprotein through which sodium enters a neuron down its concentration gradient after a moderate ('threshold') depolarization of the normal membrane potential has been achieved. The flow of sodium reaches a maximum in less than a millisecond and is usually turned off (inactivated) within several milliseconds. The local depolarization is usually lost in a somewhat longer time by the operation of an outward flow of K^+ through a potassium channel. The net imbalance in the usual intracellular K^+/Na^+ ratio is corrected after a time by the operation of the 'Na^+/K^+ pump' (Na^+/K^+ ATPase).

1.2. *Sodium channel sequence*

Superb research by Numa and his co-workers [2] has elucidated the primary structure (an 1820 amino acid sequence, calculated M_r 208321) of the sodium channel of the electric eel, *Electrophorus electricus*. The channel protein was isolated in purified form [3,4], degraded with trypsin and the resulting peptides separated and sequenced. Blot hybridization using cDNA from immunologically positive transformants with oligodesoxynucleotides corresponding to all possible variants of one of the tryptic peptides led to the isolation of a positive clone and eventually to cDNA containing the information for the channel protein. The DNA sequence was analyzed by the method of Maxam and Gilbert [5]. The Kyoto group has thoroughly analyzed the sequence, revealing genetic homologies between four sections of the protein, identifying a minimum of 12 hydrophobic helices, pointing out the four unusual positively charged sequences (and the possibility that these might be 3_{10}-helices) and noting the presence of unusual long sequences of negatively charged amino acids. A specific channel was not identified.

1.3. *Acetylcholine receptor channel*

A functional group arrangement (lys(1)...

Published by Elsevier Science Publishers B.V. (Biomedical Division)
00145793/85/$3.30

glu(4)...lys(8)... was suggested by single group rotation theory (SGR) to constitute a plausible ion channel in the acetylcholine receptor (AChR) [6]. The predicted sequence was found [7] in the amino acid sequences elucidated by Numa and others [8–12] and was utilized together with other facts and chemical logic to construct a model for the AChR [13,14]. The ion channel sequences found by SGR theory proved to be amphiphilic and were essentially the same as those identified on the basis of amphiphilic character [15,16].

2. RESULTS AND DISCUSSION

Examination of the sodium channel amino acid sequence quickly shows that no ion channel like that currently accepted for the AChR is present. The positively charged sequences noted by Numa have many hydrophobic groups interspersed with the charged groups. A charged amphiphilic sequence might be an ion channel element. I place these four sequences in the bilayer and accept the proposal by Numa [2] that the repeat period of three amino acids for these sequences would be given by a 3_{10}-helix, which is rare in proteins [17]. The apposition of charged groups in the present 3_{10}-helix is acceptable provided that additional channel elements neutralize the large number of positive charges (20+) now within the membrane. The only possibility is to insert two negatively charged segments (net 22−) into the bilayer, arranged as 3_{10}-helices on the basis of length (18 amino acids) and as a match for the positively charged helices. The functional part of the channel thus contains six 3_{10}-helices. The ion channel elements, $^{1}C^{+}$, $^{2}C^{+}$, $^{3}C^{-}$, $^{4}C^{-}$, $^{5}C^{+}$ and $^{6}C^{+}$, are shown in fig.1.

Fourteen hydrophobic α-helices were selected for dominant hydrophobic character, with the helix length limited to 24 amino acids (~36 Å). Ser, thr and cys may stabilize hydrophobic helices [18]. The choices for the hydrophobic helices agreed for the most part with those of Numa [2], but I did not rely on genetic homology to guide the distribution of such helices within the overall sequence. Six of the segments selected by Numa (I, S2,S3; II,S2,S3; III,S1,S2) as candidate amphiphilic helices were not chosen since they seemed too polar to me. The hydrophobic helices are shown in fig.2A and B. The total number of bilayer helices in our model is 20. In the AChR model, 27 bilayer helices (our model) or 25 bilayer helices (Stroud, Guy models) were proposed for 2333 amino acids. On this basis, we might expect 20 or 21 bilayer helices for the 1820 amino acids of the sodium channel.

210 arg^{+}	657 arg^{+}	1092 gly	1417 arg^{+}	910 asp^{-}	942 glu^{-}
211 thr	658 ser	1093 ala	1418 val	909 glu^{-}	943 glu^{-}
212 phe	659 leu	1094 ile	1419 ile	908 glu^{-}	944 glu^{-}
213 arg^{+}	660 arg^{+}	1095 lys^{+}	1420 arg^{+}	907 asp^{-}	945 glu^{-}
214 val	661 leu	1096 asn	1421 leu	906 ser	946 glu^{-}
215 leu	662 leu	1097 leu	1422 ala	905 ser	947 glu^{-}
216 arg^{+}	663 arg^{+}	1098 arg^{+}	1423 arg^{+}	904 asp^{-}	948 glu^{-}
217 ala	664 ile	1099 thr	1424 ile	903 val	949 glu^{-}
218 leu	665 phe	1100 ile	1425 ala	902 leu	950 glu^{-}
219 lys^{+}	666 lys^{+}	1101 arg^{+}	1426 arg^{+}	901 gly	951 pro
220 thr	667 leu	1102 ala	1427 val	900 glu^{-}	952 glu^{-}
221 ile	668 ala	1103 leu	1428 leu	899 glu^{-}	953 glu^{-}
222 thr	669 lys^{+}	1104 arg^{+}	1429 arg^{+}	898 glu^{-}	954 leu
223 ile	670 ser	1105 pro	1430 leu	897 ile	955 glu^{-}
224 phe	671 trp	1106 leu	1431 ile	896 glu^{-}	956 ser
225 pro	672 pro	1107 arg^{+}	1432 arg^{+}	895 ser	957 lys^{+}
226 gly	673 thr	1108 ala	1433 ala	894 glu^{-}	958 asp^{-}
227 leu	674 leu	1109 leu	1434 ala	893 gly	959 pro
$^{1}C^{+}$	$^{2}C^{+}$	$^{5}C^{+}$	$^{6}C^{+}$	$^{3}C^{-}$	$^{4}C^{-}$

Fig.1. Sodium ion channel elements.

141 ile	267 leu	379 met	584 ser	710 phe	767 leu	1088 tyr
140 thr	266 asn	380 val	583 met	709 leu	768 ala	1087 gly
139 met	265 gly	381 phe	582 phe	708 gln	769 val	1086 leu
138 phe	264 met	382 phe	581 leu	707 phe	770 tyr	1085 leu
137 ile	263 phe	383 ile	580 thr	706 gly	771 met	1084 ser
136 cys	262 leu	384 met	579 asn	705 val	772 met	1083 ser
135 asn	261 gln	385 val	578 leu	704 leu	773 val	1082 thr
134 ser	260 met	386 ile	577 ile	703 ala	774 ile	1081 ile
133 phe	259 gly	387 phe	576 ile	702 phe	775 ile	1080 gly
132 ile	258 ala	388 leu	575 cys	701 ile	776 ile	1079 met
131 thr	257 leu	389 gly	574 leu	700 phe	777 gly	1078 ile
130 phe	256 thr	390 ser	573 thr	699 val	778 asn	1077 ser
129 met	255 phe	391 phe	572 ile	698 ile	779 leu	1076 ala
128 ile	254 val	392 tyr	571 phe	697 ile	780 val	1075 gly
127 phe	253 ala	393 leu	570 leu	696 ala	781 met	1074 val
126 phe	252 leu	394 ile	569 asp^-	695 leu	782 leu	1073 ile
125 asn	251 ser	395 asn	568 thr	694 val	783 asn	1072 val
124 phe	250 phe	396 leu	567 phe	693 ile	784 leu	1071 phe
123 ala	249 val	397 ile	566 pro	692 thr	785 phe	1070 asp^-
122 ser	248 thr	398 leu	565 asp^-	691 leu	786 leu	1069 leu
121 asn	247 leu	399 ala	564 met	690 asn	787 ala	1068 trp
120 val	246 ile	400 val	563 met	689 gly	788 leu	1067 cys
119 phe	245 val	401 val	562 val	688 leu	789 leu	1066 trp
118 val	244 val	402 ala	561 phe	687 ala	790 leu	1065 ala
H1	H2	H3	H4	H5	H6	H7

1151 phe	1238 val	1341 val	1353 ile	1402 leu	1463 phe	1544 ile
1150 leu	1239 tyr	1340 met	1354 leu	1401 leu	1462 met	1545 thr
1149 asn	1240 met	1339 met	1355 ser	1400 leu	1461 ile	1546 phe
1148 val	1241 tyr	1338 ala	1356 gln	1399 gly	1460 leu	1547 phe
1147 gly	1242 leu	1337 val	1357 ile	1398 ile	1459 phe	1548 cys
1146 met	1243 tyr	1336 met	1358 asn	1397 ile	1458 leu	1549 ser
1145 ile	1244 phe	1335 asn	1359 val	1396 ser	1457 leu	1550 tyr
1144 ser	1245 val	1334 ile	1360 ile	1395 ile	1456 leu	1551 ile
1143 phe	1246 ile	1333 cys	1361 phe	1394 val	1455 gly	1552 ile
1142 ile	1247 phe	1332 ile	1362 val	1393 val	1454 ile	1553 leu
1141 leu	1248 ile	1331 leu	1363 ile	1392 val	1453 asn	1554 ser
1140 trp	1249 val	1330 ala	1364 ile	1391 ala	1452 phe	1555 phe
1139 phe	1250 phe	1329 met	1365 phe	1390 phe	1451 leu	1556 leu
1138 met	1251 gly	1328 ile	1366 thr	1389 asp^-	1450 ala	1557 val
1137 leu	1252 ala	1327 phe	1367 val	1388 phe	1449 pro	1558 val
1136 cys	1253 phe	1326 ile	1368 glu^-	1387 val	1448 leu	1559 val
1135 val	1254 phe	1325 asp^-	1369 cys	1386 asn	1447 ser	1560 asn
1134 leu	1255 thr	1324 thr	1370 leu	1385 trp	1446 met	1561 met
1133 leu	1256 leu	1323 phe	1371 leu	1384 gly	1445 met	1562 tyr
1132 val	1257 asn	1322 pro	1372 lys^+	1383 val	1444 leu	1563 ile
1131 asn	1258 leu	1321 gln	1373 leu	1382 thr	1443 ala	1564 ala
1130 met	1259 phe	1320 thr	1374 leu	1381 phe	1442 phe	1565 ile
1129 ile	1260 ile	1319 val	1375 ala	1380 phe	1441 leu	1566 ile
1128 ser	1261 gly	1318 ile	1376 leu	1379 tyr	1440 leu	1567 leu
H8	H9	H10	H11	H12	H13	H14

Fig.2. (A) Hydrophobic helices H1–H7. (B) Hydrophobic helices H8–H14.

The amphiphilic (+)-helices have to be in a square arrangement surrounding the completely polar (−)-helices. The interaction of the (+)-helices with the (−)-helices is maximized if the charged (mostly arginine) groups are placed between the pairs of (−) groups. The 3_{10}-helices are oriented ('outer' portion) so that the least charge faces in the direction of the hydrophobic helices. The amino acids located on the outer and inner sides (A and B) of the (−)-helices as well as those on the inner side of the (+)-helices (the side oriented towards the center) are shown in fig.3.

To minimize the number of charges in the region facing the hydrophobic portion of the channel protein, the inner sets of (−) groups are apposed to one another. The charge distributions for this arrangement are shown level by level on pentagons in fig.3. The average net charge on any side of the

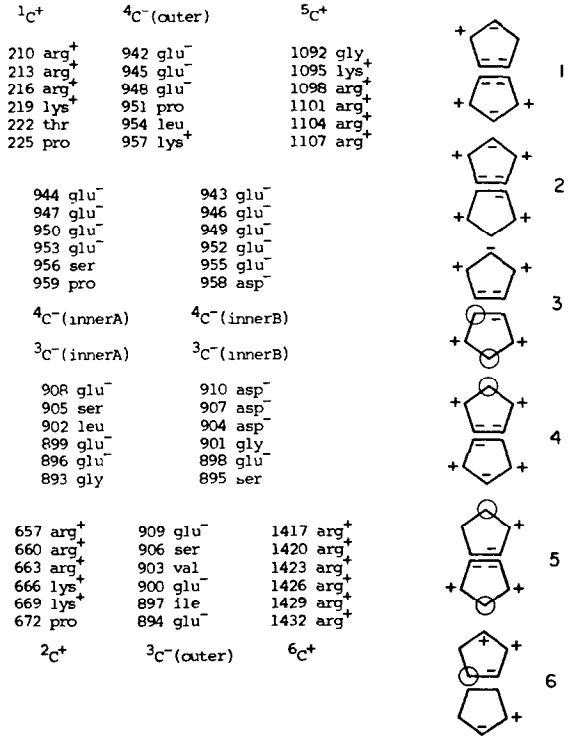

Fig.3. Ion channel active amino acids and charge distributions. The inner amino acids of the channel line the pathway which the sodium ion traverses through the bilayer. (A and B are arbitrary designations of the apposed sodium ligand groups.) The charges at each level (one turn of the 3_{10}-helix) are shown within the pentagons to the right of the amino acid lists.

combination through the bilayer ranges from −2 to +1. A significant feature of the arrangement is that the net charge at a given level of the channel changes from negative (level 1) at the top of the bilayer to positive at the bottom (level 6), the net charges being −3, 0, 0, 0, 0, 0, +1.

Thus far we have organized the sequences according to chemical logic starting with two theses. First, an ion channel should have charged groups on the channel elements. (A tight structure like that of gramicidin [19,20] does not seem feasible for a channel constructed from a number of protein helices.) Second, amphiphilic helices are excellent choices as ion channel elements.

I then applied SGR to the groups on the channel elements, in order to study what dynamic properties the channel structure might have. After single group rotation (SGR) on the (−) groups of the inner portion, I discovered that a plausible binding site for sodium was created (fig.4). The site should

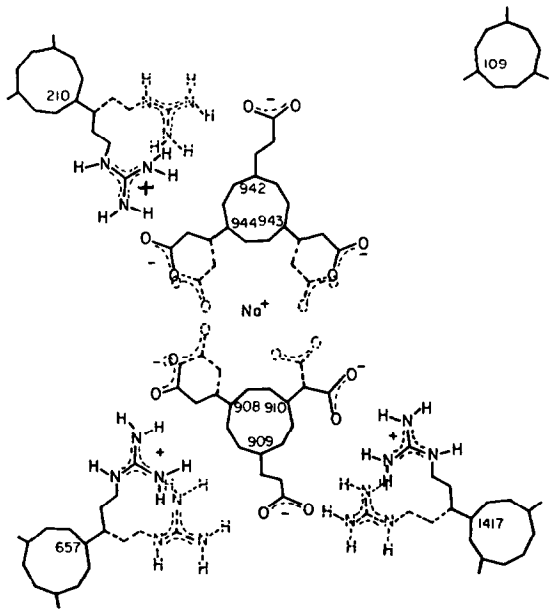

Fig.4. A representation of the level 1 arrangement of the sodium channel. The two extreme single group rotation (SGR) conformations for arginine and glutamate are indicated with dashed lines superimposed on solid lines. Two remarkable features are readily discerned. First, SGR of the glutamate side chains away from positions near the guanidino groups of arginine leads to an arrangement which looks plausible for binding a cation. Second, the guanidino groups of the arginine may interact with either the inner or outer (see fig.3) carboxylate groups according to the SGR conformation.

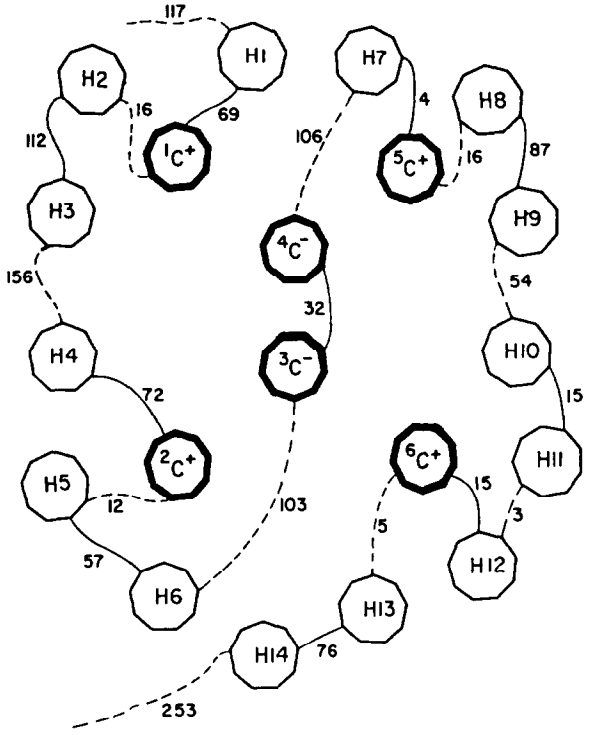

Fig.5. Schematic arrangement of the ion channel elements (fig.1) and the hydrophobic helices (H1–H14, fig.2A and B). The solid lines are connections between elements or helices outside the bilayer while dashed lines represent connections on the cytoplasmic side. The connecting links contain the indicated number of amino acids. The signs on the channel elements indicate the predominant charge on a given 3_{10}-helix. It is interesting that the top of the third channel element is amino acid 910, exactly halfway through the 1820 amino acid sequence of the channel protein.

discriminate in favor of the larger hydrated ion (Na^+) over the smaller (K^+) ion. The overall arrangement of the bilayer helices of the sodium channel is shown in fig.5. A compact representation showing the sequence numbers for the beginning and end of each bilayer helix is shown in fig.6. Seven of the potential *N*-glycosylation sites [asn-X-ser(thr)] (X not pro) at 205, 278, 288, 317, 591, 1160 and 1174 are outside the bilayer. The M_r of the glycosyl portion of the channel is ~60800 (cf. [2]).

2.1. *Channel dynamics*

An outer control element, OCE, and an inner control element, ICE, are needed to understand the operation of the sodium carrying portion of the channel. A logical choice for the OCE is the 32-amino sequence connecting the (−) ion channel elements (fig.7). This sequence contains groups of a charge type and position (941 lys^+ and/or 913 lys^+, 915 lys^+) which can block the opening to the channel and maintain a closed state. A decrease in membrane potential would allow (−) groups (e.g., 937 asp^- and/or 920 asp^-, 922 asp^-) to compete for the (+) groups which block the channel. A likely choice for the ICE would be the sequence between 793 ser and 892 lys^+. The sequence includes a substantial number of (−) groups (18^- vs 10^+), especially such sequences as those between 802 glu^- and 806 glu^- (5 (−)/5 a.a) and 847 asp^- and 857 asp^- (6 (−)/11 a.a) (fig.7).

With a normal membrane potential, (+) groups (possibly 3) from the OCE are associated with the level 1 groups of the sodium channel. The net charge on the OCE-channel complex is zero. Two extreme conformations of the OCE-channel complex are (a) expanded (no special affinity for Na^+) and (b) contracted. The latter contains a binding site for Na^+, which is readily constructed with a model for the 3_{10}-helix, and is illustrated schematically in fig.8. Depolarization, via a flow of Na^+ within the cell (either from a neighboring

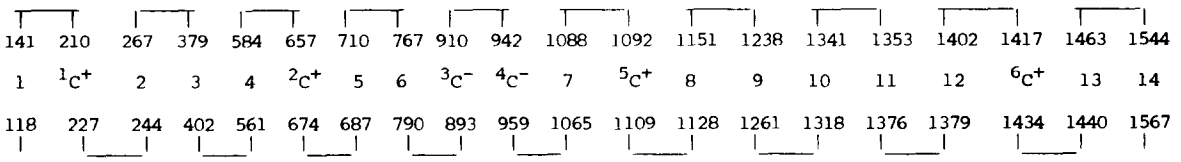

Fig.6. Compact linear representation of sodium channel organization. Number = number of transmembrane hydrophobic helix; C = ion channel element.

OCE

```
934 ser ----933 pro-----932 ser---- 931 tyr------930 asp⁻
935 glu⁻              917 ala--------918 leu     929 val
936 gln              916 his         919 asn     928 thr
937 asp⁻             915 lys⁺        920 asp⁻    927 ser
938 pro              914 lys⁺        921 glu⁻    926 cys
939 leu              913 lys⁺        922 asp⁻    925 val
940 ala              912 asn         923 ser --- 924 ser
941 lys⁺             911 thr
```

ICE

791 ser	811 gln	831 thr	851 gly	871 glu⁻	891 val
792 ser	812 val	832 val	852 glu⁻	872 lys⁺	892 lys⁺
793 phe	813 ala	833 gln	853 glu⁻	873 ile	893 gly
794 ser	814 ser	834 ala	854 gly	874 val	
795 ser	815 glu⁻	835 leu	855 asp⁻	875 asp⁻	
796 asp⁻	816 arg⁺	836 val	856 asn	876 gly	
797 asn	817 ala	837 leu	857 glu⁻	877 ile	
798 leu	818 ser	838 trp	858 gly	878 thr	
799 ser	819 arg⁺	839 ile	859 lys⁺	879 asn	
800 ser	820 ala	840 gln	860 lys⁺	880 cys	
801 ile	821 lys⁺	841 gly	861 asp⁻	881 val	
802 glu⁻	822 asn	842 lys⁺	862 thr	882 glu⁻	
803 glu⁻	823 trp	843 lys⁺	863 leu	883 ser	
804 asp⁻	824 val	844 pro	864 pro	884 pro	
805 asp⁻	825 lys⁺	845 pro	865 leu	885 thr	
806 glu⁻	826 ile	846 ser	866 asn	886 leu	
807 val	827 phe	847 asp⁻	867 tyr	887 asn	
808 asn	828 ile	848 asp⁻	868 leu	888 leu	
809 ser	829 thr	849 val	869 asp⁻	889 pro	
810 leu	830 gly	850 val	870 gly	890 ile	

Fig.7. Outer control element at entrance to sodium channel (OCE) and sequence of inner control element (ICE). The latter contains 867 tyr. If the squid axon channel has a tyrosine in a similar position, it may be the tyrosine at which *N*-bromoacetamide cleavage occurs [31].

sodium channel or from a ligand-gated channel), diminishes the attraction of the interior for the OCE. The attraction is mediated via the (+) groups moving up and the (−) groups moving down, with the outer channel region more strongly affected because of a lower dielectric constant. This charge motion can account for the gating current (motion of ~6 charges) [21,22], which would, as observed, precede channel opening [23]. The release of the OCE leads to the exposure of a potential ion-binding site, which we propose as appropriate for Na^+ (hydrated radius 2.76 Å) and somewhat less so for K^+ (hydrated radius 2.32 Å) (see discussion in section 2.2). An occupied site is shown in fig.8. The schematic sites distort the actual geometry but should faithfully reflect their character.

The binding site is metastable, in the sense that the arginine (+) charges can compete with Na^+ for the (−) charges of the ligand groups. If the ligand binding interactions decrease, the Na^+ can move to the next lower level. Inspection of the charge distributions shown on the pentagons in fig.3 show that levels 2, 3, 4 and 5 have no net charge. Thus, motion of the ions would not be retarded through most of the channel. Level 6 has a net +1 charge, which may be influenced by (−) charged groups in the cytoplasmic portion of the channel.

A maximum of 3 Na^+ can occupy the channel at levels 1, 3 and 5. The fully occupied channel will have a net 1+ charge, and can attract the ICE which then reverses the charge displacements that led to opening of the channel via dissociation of the OCE. The cloud of Na^+ which entered may

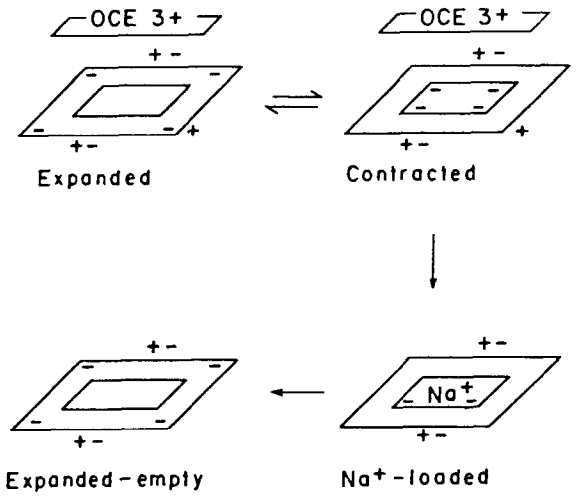

Fig.8. A schematic view of the operation of the level 1-outer control element (OCE) complex before and after acquisition of sodium ion. The expanded form of the level 1-OCE complex blocks the channel. The channel is still blocked in the contracted form, but the level 1 groups can easily combine with a sodium ion after dissociation of the OCE.

play a role in promoting conformational change within the ICE by helping to neutralize some of the negative charge. The ICE acts by helping to return the OCE to its initial state. An overall schematic equation (eqn 1) presents a summary of the channel states and the conformational changes underlying their interconversions.

Channel states

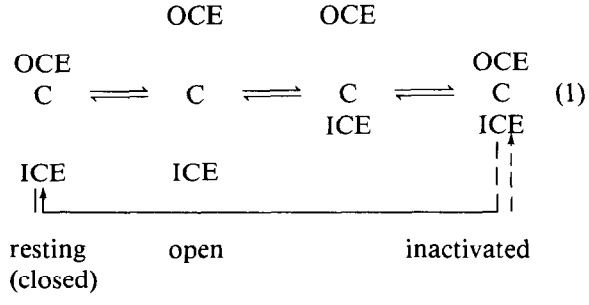

OCE, outer control element; C, sodium carrying portion of channel; ICE, inner control element.

2.2. *Toxin effects*

There are four types of sodium channel toxins, channel blockers [tetrodotoxin (TTX), saxitoxin (STX)], channel activators [batrachotoxin (BTX), grayanotoxin (GTX), veratridine, aconitine], channel inactivation blockers [scorpion, sea anemone toxins] and an activation enhancer [β-scorpion toxin] [1]. We make the tacit assumption that the effects obtained with toxins acting on sodium channels from organisms other than the eel may be used for interpretation of the *Electrophorus* channel structure [24]. Although BTX seems without effect on the sodium channels of the frog which produces it, the same channels are affected by veratridine and GTX [25]. Both TTX and veratridine act on eel channels [26].

With respect to the first type of toxins, chemical analogy suggests that tetrodotoxin (TTX) and saxitoxin (STX) act in place of the channel arginine groups at the first level, and thereby block the channel.

The lysine which we proposed [27] as a critical part of the binding site for batrachotoxin can be assigned to one or more of the groups, 941 lys^+, 913 lys^+ and 915 lys^+, in the OCE. Keeping one of these lysines out of the channel should lower the rate of inactivation. Complexation of other portions of the OCE with the other toxins can account for their activity, given the close connection between inactivation (action of the ICE?) and the operation of the OCE. The three-dimensional structure of one scorpion toxin has a triangular arrangement of charged amino acids (2 glu^-, 1 lys^+, 52 glu^-) [28] which might interact with a corresponding OCE combination (913 lys^+, 921 glu^-, 915 lys^+) with the toxin-OCE complex inhibiting closure of the channel.

Both equilibrium and kinetics play a role in determining the selectivity of the channel. The permeabilities to various ions in neuroblastoma cells and skeletal myotubes can be measured in the absence of additives ($Na^+ : K^+ : Rb^+ : (NH_2)_2C{=}NH_2^+ : CH_3NH_3^+$, 1 : 0.086 : 0.012 : 0.13 : 0.007) and in the presence of channel-opening toxins (1 : 0.4 : 0.15 : 0.65 : 0.14) [29]. Using a simple kinetic model for the passage of ions, the amount of cation delivered via the channel to the interior of a cell would be determined by the ratio of the rate at which ions pass through the channel and the rate at which inactivation occurs times an

equilibrium constant for ion binding. The more slowly the ion moves through the channel, the greater is the inactivation rate. In the presence of toxins, the OCE-toxin complex forms, inactivation does not occur, and the 'intrinsic rates' of cation diffusion through the channel would control the amount of cation going through the membrane (see eqn 1).

2.3. *Effects of other agents*

Methylation of carboxylate groups of frog nodes of Ranvier with trimethyloxonium ion leads to the loss of TTX-sensitivity and a lower channel conductance [30], a finding consistent with the present model. The removal of sodium channel inactivation by the internal perfusion of squid axons with *N*-bromoacetamide has been ascribed to cleavage of a peptide link next to tyrosine [31]. Cleavage of the ICE at 867 tyr would interfere with the conformational change needed to initiate inactivation. Internal perfusion of squid axons with pronase, a nonspecific peptidase, removes sodium channel inactivation [32], as expected for partial or complete removal of the ICE. The reappearance of inactivation (lost after pronase treatment) through introduction of polyglycylarginine [33] or octylguanidinium ion [34] suggests that a polypeptidic or hydrophobic guanidinium ion can simulate the action of the ICE. Some interaction of Ca^{2+} with the binding site can account for the calcium-induced decrease in sodium conductance [35].

2.4. *Phosphorylation*

Modification of the sodium channel by phosphorylation has been demonstrated in several preparations. Candidate sites for labeling are 883 ser, 885 thr, 964 thr or 979 thr.

Proline distribution: Unusual concentrations of proline at the ends of the AChR β, γ and δ-subunits have been noted and may be associated with an intracellular anchor [14]. In this connection, we note that two intracellular regions of the sodium channel have unusually high proline contents, e.g., 54–70 (5 pro/17 a.a) and 1772–1788 (5 pro/17 a.a). Of 74 prolines in the channel, our model assigns 7 to the bilayer, 21 to the exocyclic and 46 to the cytoplasmic portions of the protein.

2.5. *Mass distribution*

In the proposed model, the sodium channel is evenly distributed between the outside (46.7%) and inside (47.4%) of the cell, with a minor fraction (5.9%) within the bilayer.

3. CONCLUSIONS

The sodium channel is one of the few channels for which there is a structural idea about how the ions traverse the membrane bilayer. Others are gramicidin, alamethicin and the acetylcholine receptor. Each channel is built on a completely different plan. The evolutionary stability of the AChR is known [36–38], while that of the Na^+ channel remains to be seen. The rat brain sodium channel contains a major polypeptide (M_r 260000) and two additional peptides with M_r of 37000 and 39000 [39]. The structure of the K^+ and Ca^{2+} channels will help us perceive a pattern, if any, in channel design.

The sodium channel model proposed here is a remarkably balanced and beautiful structure, which deserves the comment, "Si non e vero, e ben trovato". The structural features discovered with the model may well deserve incorporation into a synthetic model. In addition, these features are a chemical expression of a new physical model for channel gating [40], and define a molecular basis for local anesthetic blocking of the open channel [41].

REFERENCES

[1] Catterall, W.A. (1984) Science 223, 653–661; Witkop, B. (1982) Heterocycles 17, 431–445.
[2] Noda, M., Shimizu, S., Tanabe, T., Takai, T., Kayano, T., Ikeda, T., Takahashi, H., Nakayama, H., Kanaoka, Y., Minamino, N., Kangawa, K., Matsuo, H., Raftery, M.A., Hirose, T., Notake, M., Inayama, S., Hayashida, H., Miyata, T. and Numa, S. (1984) Nature 312, 121–127.
[3] Agnew, W.S., Levinson, S.R., Brabson, J.S. and Raftery, M.A. (1978) Proc. Natl. Acad. Sci. USA 75, 2606–2610.
[4] Nakayama, H., Withy, R.M. and Raftery, M.A. (1982) Proc. Natl. Acad. Sci. USA 79, 7575–7579.
[5] Maxam, A.M. and Gilbert, W. (1980) Methods Enzymol. 65, 499–560.
[6] Kosower, E.M. (1982) Abstracts pp.52–53, Int. Sympos. Structure and Dynamics of Nucleic Acids and Proteins', La Jolla, CA, 5–9 September.
[7] Kosower, E.M. (1983) Biochem. Biophys. Res. Commun. 111, 1022–1029.

[8] Noda, M., Takahashi, H., Tanabe, T., Toyosato, M., Furutani, Y., Hirose, T., Asai, M., Inayama, S., Miyata, T. and Numa, S. (1982) Nature 299, 793–797.
[9] Noda, M., Takahashi, H., Tanabe, T., Toyosato, M., Kikyotani, S., Hirose, T., Asai, M., Takashima, H., Inayama, S., Miyata, T. and Numa, S. (1983) Nature 301, 251–255.
[10] Noda, M., Takahashi, H., Tanabe, T., Toyosato, M., Kikyotani, S., Furutani, Y., Hirose, T., Takashima, H., Inayama, S., Miyata, T. and Numa, S. (1983) Nature 302, 528–532.
[11] Claudio, T., Ballivet, M., Patrick, J. and Heinemann, S. (1983) Proc. Natl. Acad. Sci. USA 80, 1111–1115.
[12] Devillers-Thiery, A., Giraudat, J., Bentaboulet, M. and Changeux, J.-P. (1983) Proc. Natl. Acad. Sci. USA 80, 2067–2071.
[13] Kosower, E.M. (1984) FEBS Lett. 172, 1–5.
[14] Kosower, E.M. (1985) submitted.
[15] Finer-Moore, J. and Stroud, R.M. (1984) Proc. Natl. Acad. Sci. USA 81, 155–159.
[16] Guy, H.R. (1984) Biophys. J. 45, 249–261.
[17] Schulz, G.E. and Schirmer, R.H. (1979) Principles of Protein Structure, pp.70–71.
[18] Gray, T.M. and Matthews, B.W. (1984) J. Mol. Biol. 175, 75–81.
[19] Urry, D.W. (1972) Proc. Natl. Acad. Sci. USA 69, 1610–1614; (1979) Int. Rev. Neurobiol. 21, 311–334.
[20] Mackay, D.H.J., Berens, P.H., Wilson, K.R. and Hagler, A.T. (1984) Biophys. J. 45, 229–248.
[21] Armstrong, C.M. and Bezanilla, F. (1974) J. Gen. Physiol. 63, 533–552.
[22] Kuffler, S.W., Nicholls, J.G. and Martin, A.R. (1984) From Neuron to Brain, 2nd edn, pp.157–160, Sinauer Associates, Sunderland, MA.
[23] French, R.J. and Horn, R. (1983) Annu. Rev. Biophys. Bioeng. 12, 319–356.
[24] Barchi, R.L. (1982) Int. Rev. Neurobiol. 23, 69–101.
[25] Daly, J.W., Myers, C.W., Warnick, J.E. and Albuquerque, E.X. (1980) Science 208, 1383–1385.
[26] Rosenberg, R.L., Tomiko, S.A. and Agnew, W.S. (1984) Proc. Natl. Acad. Sci. USA 81, 1239–1243.
[27] Kosower, E.M. (1983) FEBS Lett. 163, 161–164.
[28] Fontecilla-Camps, J.C., Almassy, R.J., Suddath, F.L., Watt, D.D. and Bugg, C.E. (1980) Proc. Natl. Acad. Sci. USA 77, 6496–6500.
[29] Frelin, C., Vigne, P. and Lazdunski, M. (1981) Eur. J. Biochem. 119, 437–442.
[30] Sigworth, F.J. and Spalding, B.C. (1980) Nature 283, 293–295.
[31] Oxford, G.S., Wu, C.H. and Narahashi, T. (1978) J. Gen. Physiol. 171, 227–247.
[32] Armstrong, C.M., Bezanilla, F. and Rojas, E. (1973) J. Gen. Physiol. 62, 375–391.
[33] Eaton, D.C., Brodwick, M.S., Oxford, G.S. and Rudy, B. (1978) Nature 271, 473–476.
[34] Oxford, G.S. and Yeh, J.Z. (1982) Biophys. J. 37, 104a.
[35] Yamamoto, D., Yeh, J.Z. and Narahashi, T. (1984) Biophys. J. 45, 337–344.
[36] Noda, M., Furutani, Y., Takahashi, H., Toyosato, M., Tanabe, T., Shimuzu, S., Kikyotani, S., Kayano, T., Hirose, T., Inayama, S., Miyata, T. and Numa, S. (1983) Nature 305, 818–823.
[37] Takai, T., Noda, M., Furutani, Y., Takahashi, H., Notake, M., Shimizu, S., Kayano, T., Tanabe, T., Tanaka, K., Hirose, T., Inayama, S. and Numa, S. (1984) Eur. J. Biochem. 143, 109–115.
[38] Tanabe, T., Noda, M., Furutani, Y., Takai, T., Takahashi, H., Tanaka, K.-I., Hirose, T., Inayama, S. and Numa, S. (1984) Eur. J. Biochem. 144, 11–17.
[39] Hartshorne, R.P. and Catterall, W.A. (1984) J. Biol. Chem. 259, 1667–1675.
[40] Finkelstein, A. and Peskin, C.S. (1984) Biophys. J. 46, 549–558.
[41] Starmer, C.F., Grant, A.O. and Strauss, H.C. (1984) Biophys. J. 46, 15–27.